# Dalton Transactions

Accepted Manuscript






ROYAL SOCIETY OF CHEMISTRY

www.rsc.org/dalton

Journal Name

ARTICLE

# Catalytically Active Lead(II)-Imidazolium Coordination Assemblies with Diversified Lead(II) Coordination Geometries

Received 00th January 20xx,
Accepted 00th January 20xx

DOI: 10.1039/x0xx00000x

www.rsc.org/

Chatla Naga Babu,[a] Paladugu Suresh,[a] Katam Srinivas,[a] Arruri Sathyanarayana,[a] Natarajan Sampath[b] and Ganesan Prabusankar[a*]

Five Pb(II)-imidazolium carboxylate coordination assemblies with novel structural motifs were derived from the reaction between corresponding flexible, semi flexible or rigid imidazolium carboxylic acid ligands and lead nitrate. The imidazolium linker present in these molecules likely plays a triple role such as a counter ion to balance the metal charge, a ligand being an integral part of the final product and a catalyst facilitating carbon-carbon bond formation reaction. These lead-imidazolium coordination assemblies exhibit , variable chemical and thermal stability, as well as catalytic activity. These newly prepared catalysts are highly active towards benzoin condensation reactions with good functional group tolerance.

## Introduction

Carboxylate functionalized imidazolium organic spacers have proved to be one of the most promising chelating ligands due to their extraordinary binding affinity toward most metal ions, together with the pre-N-heterocyclic carbene (NHC) centres for the wide range of applications including fuel cell,[1] gas storage,[1-3] and catalysis.[3-7] As demonstrated for MOFs, the pre and post-modified NHC-MOF allows multiple catalytic sites within close proximity to access into its homogeneous counterpart (NHC based catalysts) of heterogeneous catalysts. However, the pre and post-modifications at imidazolium-MOF are the most challenging task. Very few attempts have been made to realize the catalytic activities of pre and post-modified NHC-MOFs. The first catalytic application of NHC-MOF, $Cu(R)_{0.24}(R)_{0.76}Pd_{0.76}(H_2O)_4(NO_3)_2$, R = 1,1'-methylenebis(3-(4-carboxyphenyl)-1*H*-imidazol-3-ium), by anchoring palladium through post-modified route for Suzuki–Miyaura cross-coupling reaction of phenylhalides and phenylboronic acids was demonstrated by Kong *et al.*.[4] Later palladium(II) anchored NHC-MOF, $[ZnR'_{0.42}R'_{0.58}Cl_2Pd_{0.58}(H_2O)_{1.16}]\cdot 9H_2O$, R' = 1,1'-methylenebis(3-(4-carboxy-2-methylphenyl)-1*H*-imidazol-3-ium) was reported through post-modified route for Heck coupling of aryl halides with olefins, hydrogenation of olefins and reduction of nitrobenzene for the formation of aniline.[5] Recently, Burgun *et al.* reported the first $[Zn_4O\{Cu(R'')_2\}_2]$, R'' = 1,3-bis(4-carboxyphenyl)imidazolium, using pre-modified $[Cu(R'')_2]$ spacer for hydroboration of carbondioxide.[6] Subsequently, Lalonde *et al.* developed the first *N*-heterocyclic carbene-like (organocatalyst like) catalyst $[Co_3Cl_6(R'')_2]$, R'' = 1,3,5-trimethylimidazole-2,4,6-triethylbenzene. Base, *n*-butyl lithium was used to deprotonate imidazolium proton at $[Co_3Cl_6(R'')_2]$. The deprotonated NHC-MOF, $[Co_3Cl_6(R'')_2]$ showed the efficient conversion of $\alpha,\beta$-unsaturated ketone to the corresponding methyl ether compared to homogeneous NHC catalysts.[7] Notably, the similar such catalytic activities using maingroup metal NHC-MOF's have never been demonstrated as of now. In this paper we report the first lead(II) imidazolium coordination polymers mediated benzoin condensation reactions. In contrast to Lalonde *et al.* methodology,[7] in this work we used potassium *tert*butoxide salt as deprotonation base to activate lead(II) imidazolium coordination polymers. These newly prepared catalysts are highly active towards benzoin condensation reactions with good functional group tolerance.

## Results and discussion

Among known imidazolium carboxylate supported coordination assemblies,[1-7] the heavier p-block metal coordination polymers are scarce due to the formation of ill-defined insoluble materials. In particular the heavier p-block metals are expected to depict the interesting topological arrangements and unexpected coordination geometries due to their wide range of coordination numbers. The only example known upto now with imidazolium carboxylate is chiral doubly folded interpenetrating 3D Pb(II)-imidazolium carboxylate frame work, $[PbCl[\{HCN(CH_2COO)\}_2CH]_n$, which was constructed from the reaction between flexible zwitterionic imidazolium carboxylate spacer **L**$H_2Cl$ (Chart 1) and $Pb(NO_3)_2$ at ambient temperature in aqueous solution.[8] Although Pb(II)-imidazolium carboxylates have the potential to fabricate novel

[a] *Department of Chemistry, Indian Institute of Technology Hyderabad, Kandi, Medak, Telangana, INDIA-502 285. Fax: +91 40 2301 6032; Tel: +91 40 2301 6089; E-mail: prabu@iith.ac.in.*
[b] *School of Chemical and Biotechnology, SASTRA University, Tirumalaisamudram, Thanjavur, Tamil Nadu, INDIA-613 401.etc.*
† Footnotes relating to the title and/or authors should appear here.
Electronic Supplementary Information (ESI) available: [$^1$H NMR, $^{13}$C NMR, FT-IR, Solid-state fluorescence spectra and Table S1-S3]. See DOI: 10.1039/x0xx00000x

structural motif with possible applications, importance of these derivatives in catalysis or gas storage applications have not been reported yet. Therefore as listed in chart 1, we presumed that the structurally modified imidazolium carboxylates with higher or lower degrees of flexibility and suitable reaction conditions can led to the structurally well characterized lead-imidazolium carboxylates. In this paper, we report five new, $[Pb(\mathbf{L})(NO_3)]_n$ (**1**), $[Pb_5(\mathbf{L^1})_2(NO_3)_2(Br)_{4.4}(Cl)_{2.6}(H_2O)]_n{\cdot}(NO_3)_2{\cdot}xH_2O$ (**2**), $[Pb_4(\mathbf{L^2})_2(NO_3)_8(H_2O)_4]_n{\cdot}xH_2O$ (**3**), $[Pb(\mathbf{L^3})(Cl)]_n$ (**4**) and $[Pb(\mathbf{L^3})(NO_3)]_n$ (**5**), lead(II) imidazolium coordination assemblies from the reaction between $Pb(NO_3)_2$ and different imidazolium carboxylate ligands with flexible (**LH**),[8] semi flexible ($\mathbf{L^1}H_2Br_2$ and $\mathbf{L^2}H_2Br_2$)[4] and rigid ($\mathbf{L^3}H_2Cl$)[1] coordination arms (Chart 1). **1** and **3-5** are insoluble in most of the common solvents, while **2** is soluble only in DMSO and hot water. The solubility of **2** may be attributed to the presence of more organic moieties present in the complexes compare to other complexes. **1-5** were characterized by FT-IR, solid-state UV-vis, solid-state fluorescent spectroscopy, thermogravimetric analysis and single crystal X-ray diffraction techniques.

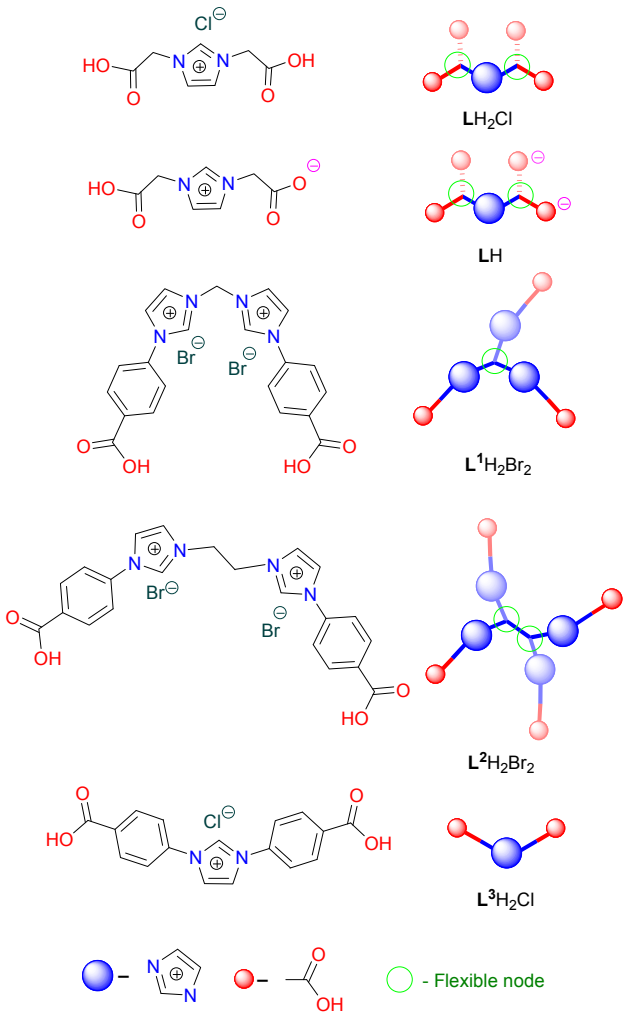


**Chart 1.** Flexible, semi flexible and rigid imidazolium carboxylate ligands used in the present study.

**Synthesis and characterization of 1**

The molecule **1** was obtained from the reaction between zwitterionic **LH** and $Pb(NO_3)_2$ in DMF. The FT-IR spectrum of **1** shows the characteristic frequency at 1642 $cm^{-1}$ and 1555 $cm^{-1}$ for monodentately coordinated carboxylate groups. The stretching frequency at 1389 $cm^{-1}$ and 1308 $cm^{-1}$ confirms the presence of bidentate $NO_3^-$ moiety.[9]

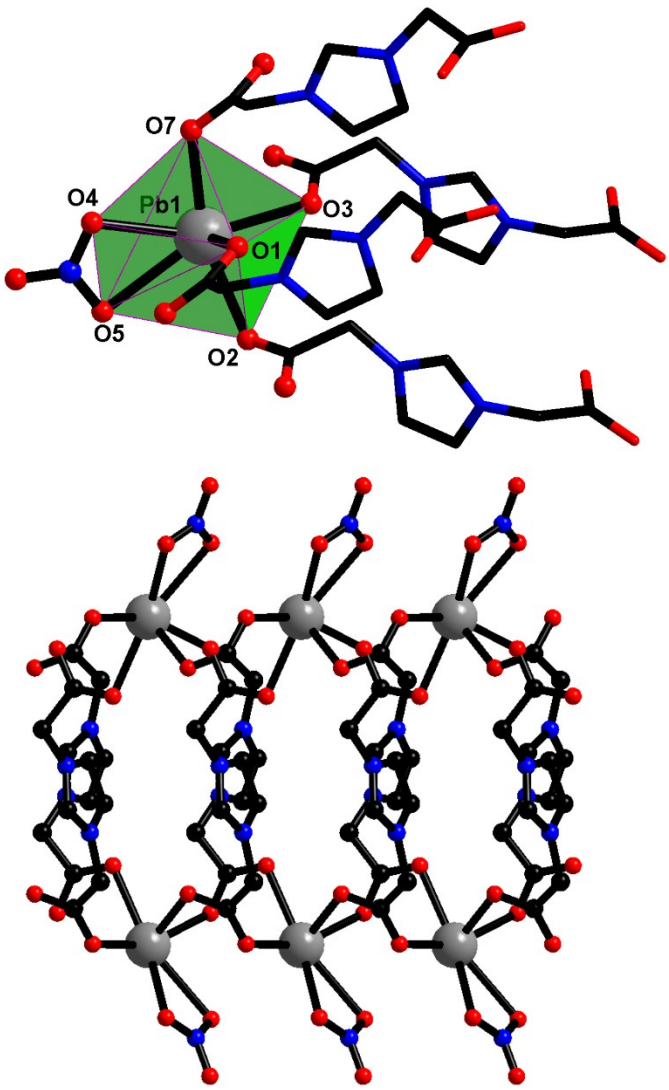


**Fig 1.** Top: The distorted pentagonal pyramidal geometry of lead(II) in **1**. Bottom: Views of the 2D structure of **1** down the c-axis emphasizing 20-member metallacyclic ring.

The solid state structure of **1** was further confirmed by single crystal X-ray diffraction study (Fig. 1). Molecule **1** crystallized in the monoclinic space group, *P2₁/c* (Table 1). *The* asymmetric unit of **1** consisting of lead atom, ligand and coordinated $NO_3^-$ moiety. Molecule **1** is a two dimensional coordination polymer, where each lead centre is bridged by four ligands. Each lead atom is six-coordinated by four oxygen atoms of four carboxylate groups and two oxygen atoms of $NO_3^-$ ion. The geometry of lead can be described as distorted pentagonal pyramidal geometry. The $Pb–O_2NO$ bond lengths are not

comparable (Pb(1)–O(5), 2.652(7) Å and Pb(1)–O(5), 2.865(7) Å). The O–Pb–$ONO_2$ angle is 46.04(2)°. The Pb–$O_{carboxylate}$ bond lengths are in the range between 2.412(7) Å to 2.568(7) Å. The Pb–O bond distances observed in **1** are comparable to those observed in the related complex $[PbCl[\{HCN(CH_2COO)\}_2CH]_n$.[8] The monodendate mode of carboxylate coordination in **1** is further evidenced by the $_{carboxylate}O–Pb–O_{carboxylate}$ angles, which is comparable with that of $[PbCl[\{HCN(CH_2COO)\}_2CH]_n$.[8]

**Synthesis and characterization of 2**

Compound **2** was prepared from the reaction between $\mathbf{L^1}H_2Br_2$ and $Pb(NO_3)_2$ in water. In FT-IR spectrum the bidentately coordinating carboxylate groups appeared at 1696 $cm^{-1}$, 1647 $cm^{-1}$ and 1607 $cm^{-1}$, while bridging $NO_3^-$ ions observed at 1549 $cm^{-1}$, 1422 $cm^{-1}$, 1394 $cm^{-1}$ and 1343 $cm^{-1}$.[9] In $^1$H NMR, the N–C*H*–N proton appeared at $\delta$ 10.20 ppm. The $^{13}$C NMR chemical shift value of *C*–O and N–*C*H–N carbons are detected at $\delta$ 166.9 and 137.9 ppm, respectively.

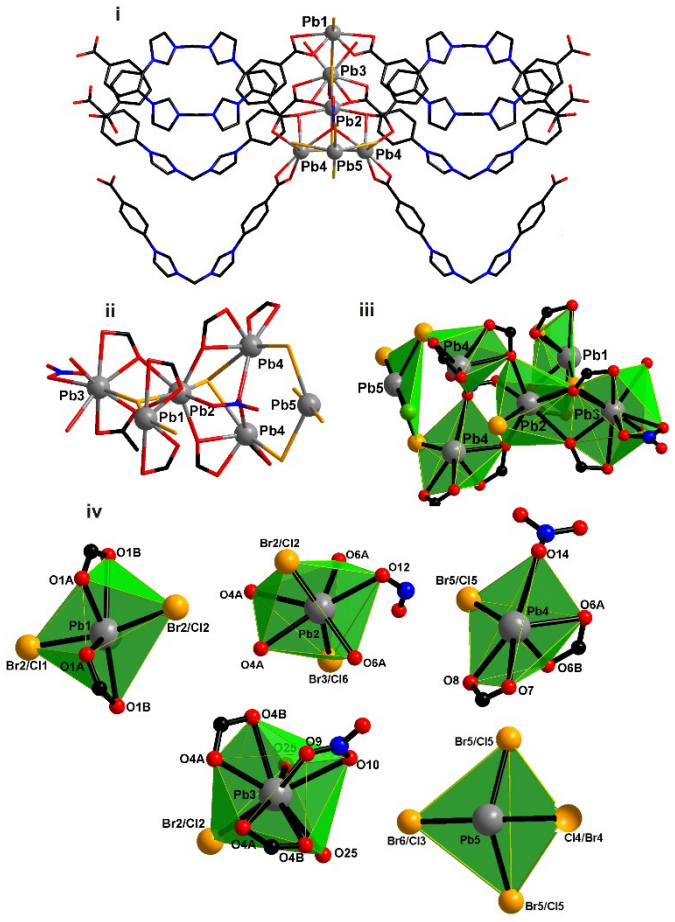


**Fig 2.** (i) The solid state structure of **2** showing orientation of hexa nuclear lead cluster. Anions, hydrogen atoms and water molecules have been omitted for clarity. (ii) Core structure of hexa nuclear lead cluster. (iii) Polyhedral sharing of hexa nuclear lead cluster. (iv) The geometry of lead(II) centres in **2**.

Molecule **2** is a rare three dimensional lead carboxylate coordination polymer constructed by hexa-nuclear lead cluster (Fig. 2; Table 1). The hexa-nuclear lead clusters are further integrated through $\mathbf{L^1}$ and Br···H–C hydrogen bonding to form a three dimensional lead carboxylate coordination polymer (Fig. 2(i)). Interestingly, each lead centre in **2** depicts different coordinated geometry (Fig 2 (ii, iii and iv)). Pb(1) and Pb(4) are hexacoordinated, while Pb(2) is heptacoordinated. Pb(5) is pentacoordinated, while Pb(4) is octacoordinated. Pb(3) is nonacoordinated. The geometry of lead centres in **2** are not comparable. The coordination environment of Pb(1) is fulfilled by four carboxylate oxygen atoms and two Br/Cl ions. The Pb(2) is surrounded by four monodentately coordinated carboxylate oxygen atoms, two Br/Cl ions and one nitrate ion. The geometry of Pb(3) is satisfied by four carboxylate oxygen atoms, two oxygen atoms of nitrate ions, two oxygen atoms of water molecules and one Br/Cl ion. The coordination environment of Pb(4) is accomplished by four carboxylate oxygen atoms, three Br/Cl ions and one oxygen atoms of nitrate ion. The coordination environment of Pb(5) is satisfied by four bromide ions and one oxygen atoms of nitrate ion. The hexanuclear lead-oxo-bromo cluster based lead coordination polymer with different geometrical arrangement is very rare. The charge of four $Pb^{2+}$ centers are balanced by six $NO_3^-$ ions and remaining two positive charges may be balanced by disordered two $NO_3^-$ ions, which are unclear since we eliminated by PLATON SQUEEZE. Pb–Br bond distance varies from 2.822(2) Å to 3.229(16) Å and Pb–Cl bond distance varies from 2.822(2) Å to 3.050(2) Å. The shortest Pb–O bond distance is found for Pb(1)–O(1) (2.311(7) Å), while the longest Pb–O bond distance is observed for Pb(4)–O(6A) (2.732(7) Å). The Br is contaminated by Cl. The relative contributions of Cl and Br is 4.4 Br to 2.6 Cl per formula unit. The source for chloride in **2** could be the ligand because ligand was derived from its ester using concentrated hydrochloric acid.

**Synthesis and characterization of 3.**

The colourless crystals of **3** was isolated from the reaction between $\mathbf{L^2}H_2Br_2$ and $Pb(NO_3)_2$ in water and DMF solution. The FT-IR spectrum of **3** showed a characteristic peak at 1601 $cm^{-1}$ for the asymmetric ($CO_2^-$) and symmetric ($CO_2^-$) stretching vibrations of carboxylate groups. The bridging $NO_3^-$ ions appeared at 1531 $cm^{-1}$ and 1386 $cm^{-1}$.[9] The solid state structure of **3** was further confirmed by single crystal X-ray diffraction (Fig. 3). Molecule **3** crystallized in the monoclinic space group, $P2_1/n$ (Table 1). **3** is an interpenetrated two dimensional coordination polymer (Fig. 3(iv) and 3(v)). Molecule is constituted by tetra nuclear lead centres linked through two $\mathbf{L^2}$ ligands (Fig. 3(i)) (See supporting information 1, fig. S10 for charge balance). The geometry and coordination types of lead centres are not comparable (Fig. 3(ii)). Pb(1) and Pb(2) are six coordinated, Pb(3) is nine coordinated, while Pb(4)/Pb(5) are four coordinated. Pb(3) is in distorted mono caped pentagonal bipyramid geometry. The geometry of Pb(2) can be considered as distorted pentagonal pyramid. Pb(1) is in distorted mono caped square planar geometry, while Pb(4)/Pb(5) is in distorted square pyramid geometry. Carboxylate ligand $\mathbf{L^2}$ is bidentately coordinating to lead centre, where by it bridges the lead centres. Notably, $NO_3^-$ anions show monodentate, bidentate and tridentate

coordination modes. The bidentate $NO_3^-$ anions depict both bridging and non-bridging mode of coordination, while $NO_3^-$ anion exist in bridging tridentate coordination mode (Fig. 3(iii)). The Pb–O bond distances are in the range from 2.383(14) Å (Pb(2)–O(26)) to 2.723(17) Å (Pb(2)–O(23)). The O–Pb–O angles varies from 49.8(3)° (O(11)–Pb(3)–O(10)) to 144.8(4)° (O(11)–Pb(3)–O(19)).

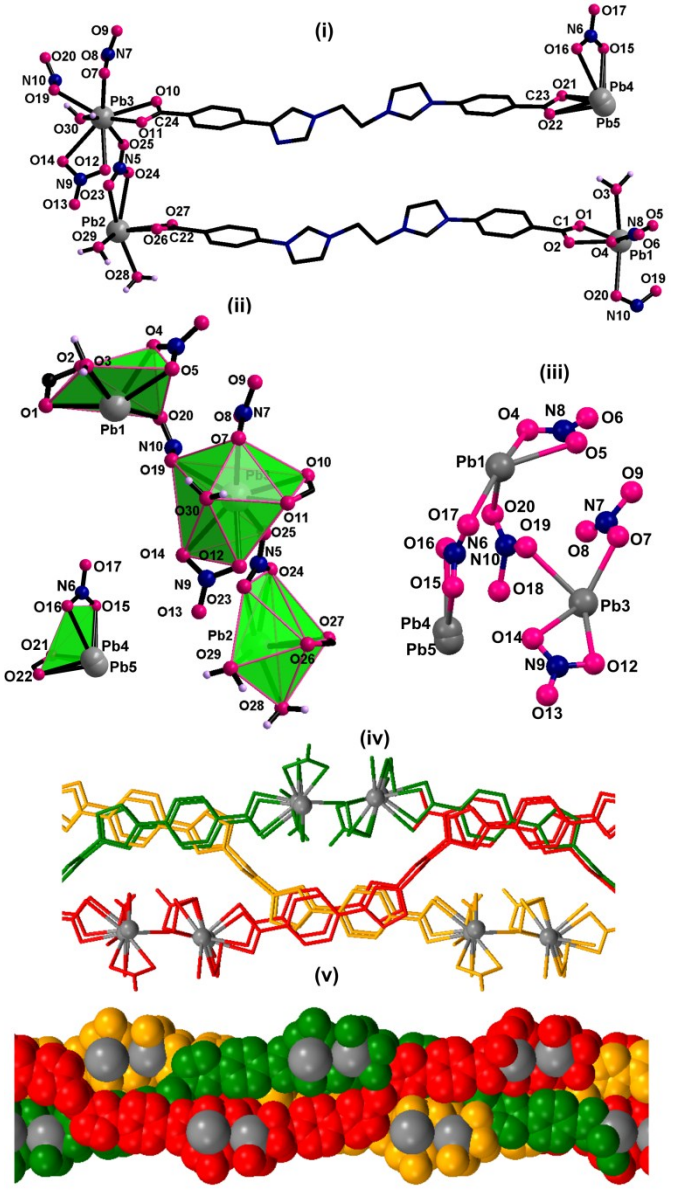


**Fig 3.** (i) Coordination mode of $L^2$ in **3**. Hydrogen atoms and water molecules have been omitted for clarity. Hydrogen atoms ligands have been omitted for clarity. (ii) Geometry of nine, six and five coordinated lead centres, (iii) Tetera nuclear core structure of **3** showing orientation of nine, six and five coordinated lead centres, (iii) Interpenetrated triple layers in **3**. View along a axis. Hydrogen atoms and water molecules have been omitted for clarity, (iv) Space filling model of triple helix like structure. View along a axis. Hydrogen atoms and water molecules have been omitted for clarity.

**Synthesis and characterization of 4.**

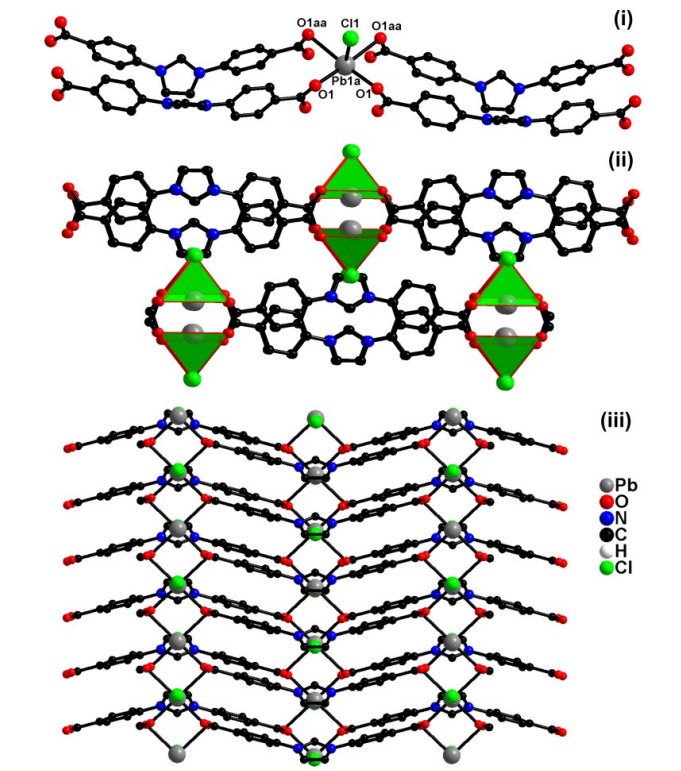


**Fig 4.** (i) Coordination mode of $L^3H_2Cl$ in **4**. (ii) Polyhedron arrangements of five coordinated lead centre in **4**, Hydrogen atoms have been omitted for clarity. (iii) Slipped layers in **4**. View along c axis. Hydrogen atoms have been omitted for clarity.

The molecule **4** was obtained from the reaction between $L^3H_2Cl$ and $Pb(NO_3)_2$ in DMF at 120 °C for 12 h under solvothermal condition. The FT-IR spectrum of **4** showed the characteristic stretching vibrations at 1598 $cm^{-1}$ and 1538 $cm^{-1}$ for carboxylate groups.[9] The solid state structure of **4** is further confirmed by single crystal X-ray diffraction technique (Fig. 4). Compound **4** crystallized in the orthorhombic space group, *Cmc2₁* (Table 1). Lead centre is penta coordinated with square pyramid geometry (Fig. 4(i) and 4(ii)). The geometry of lead is satisfied by four carboxylate oxygen atoms and one chloride ligand. The four carboxylate oxygen atoms and lead are in the same plane, while chloride occupies the pyramidal position. As shown in figure 4(ii) carboxylates are bidentately bridging between two lead centres. Each $L^3$ is linked with four lead centres. As a result, **4** consist of two dimensional slipped layers (Fig. 4(iii)). The Pb–O bond lengths are comparable (2.420(6) Å). The O–Pb–O angles are comparable 92.1(3)°.

**Synthesis and characterization of 5.**

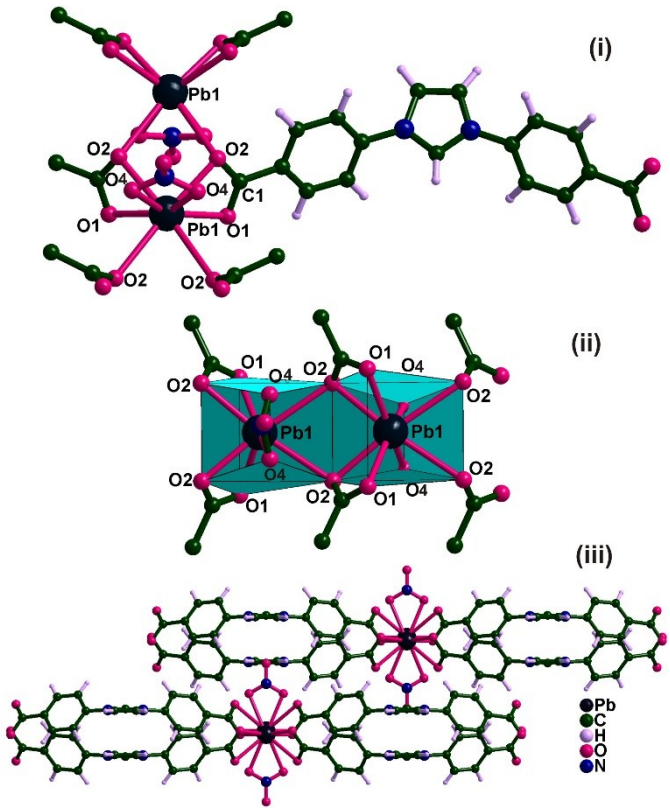


**Fig 5.** (i) Coordination mode of $L^3H_2Cl$ in **5**. (ii) Polyhedron arrangement of eight coordinated lead centre in **5**. (iii) Slipped two dimensional layers in **5**. View along c axis.

The molecule **5** was obtained from the modified reaction condition of **4** (See supporting information, Fig. S11). The colourless crystals of **5** were derived from the reaction between $L^3H_2Cl$ and $Pb(NO_3)_2$ in DMF at 120 $^oC$ for two days. The FT-IR spectrum of **5** showed the characteristic stretching frequencies at 1608 $cm^{-1}$, 1579 $cm^{-1}$ and 1545 $cm^{-1}$ for the carboxylate groups. The bidentate $NO_3^-$ ions appeared at 1512 $cm^{-1}$, 1430 $cm^{-1}$, 1353 $cm^{-1}$ and 1312 $cm^{-1}$.[9] The solid state structure of compound is further confirmed by single crystal X-ray diffraction technique (Fig. 5). Compound **5** crystallized in the orthorhombic space group, *Pnma* (Table 1). Molecule **5** can be described as two dimensional coordination layers, where each lead centre is bridged by two $L^3$ ligands (Fig. 5(i)). Each lead atom is eight coordinated by six carboxylate oxygen atoms and two $NO_3^-$ oxygen atoms. The geometry of lead centres can be described as distorted cube (Fig. 5(ii)). The $NO_3^-$ moiety is bidentately coordinating to each Pb centre. Each carboxylate group is tridentately coordinating with two Pb centres to form a slipped two dimensional coordination layers. The Pb–O(carboxylate) bond lengths are not comparable 2.601(10) Å (for Pb(1)–O(1)) to 2.470(15) Å (for Pb(1)–O(2)). Pb–O($NO_2$) bond lengths are comparable (2.76(2) Å). The O(1)–Pb(1)–O(2) angle is in the range of 108.5(4)$^o$.

**Table 1**. Structural parameters of **1**-**5**.

| Compounds | 1 | 2 | 3 | 4 | 5 |
|---|---|---|---|---|---|
| Empirical formula | $C_7H_7N_3O_7Pb$ | $C_{84}H_{64}Br_{4.7}Cl_{2.3}N_{18.5}O_{35}Pb_6$ | $C_{44}H_{44}N_{14}O_{30}Pb_4$ | $C_{17}H_{11}ClN_2O_4Pb$ | $C_{17}H_{11}N_3O_6Pb_1$ |
| Formula weight | 452.35 | 3594.47 | 2077.69 | 549.93 | 560.48 |
| T (K) | 150 | 150 | 293 | 150 | 150 |
| Crystal system | Monoclinic | orthorhombic | monoclinic | orthorhombic | orthorhombic |
| Space group | $P2_1/c$ | $Pnma$ | $P2_1/n$ | $Pnma$ | $Cmc2_1$ |
| $a$/Å | 4.53465(10) | 31.6333(7) | 14.0229(6) | 7.3476(4) | 17.2038(9) |
| $b$/Å | 20.2191(6) | 19.2972(5) | 24.1691(7) | 17.9122(8) | 11.4575(6) |
| $c$/Å | 11.4766(3) | 19.7693(5) | 19.4086(7) | 12.0710(6) | 8.4614(4) |
| α/° | 90 | 90 | 90 | 90 | 90 |
| β/° | 97.340(3) | 90 | 109.221(4) | 90 | 90 |
| γ/° | 90 | 90 | 90 | 90 | 90 |
| V (Å$^3$) | 1043.62(5) | 12067.9(5) | 6211.3(4) | 1588.68(14) | 1667.85(15) |
| $Z$ | 4 | 4 | 4 | 4 | 4 |
| $\rho_{calc}$/mg $mm^{-3}$ | 2.879 | 1.978 | 2.222 | 2.299 | 2.232 |
| $\mu$ ($mm^{-1}$) | 31.843 | 18.906 | 21.556 | 22.443 | 20.069 |
| $F$(000) | 832.0 | 6695.0 | 3896.0 | 1032.0 | 1056.0 |
| Data collected | 3501 | 11648 | 11561 | 3715 | 2042 |
| Unique data | 1966 | 11648 | 11561 | 1553 | 1206 |
| $R_{int}$ | 0.0492 | 0.570 | 0.0848 | 0.0273 | 0.0211 |
| GOF on $F^2$ | 1.074 | 0.972 | 0.950 | 1.058 | 1.071 |
| $R_1$ ($I>2\sigma(I)$) | 0.0726 | 0.0475 | 0.0715 | 0.0514 | 0.0439 |
| w$R_2$ ($I>2\sigma(I)$) | 0.1886 | 0.1252 | 0.1790 | 0.1356 | 0.1185 |
| $R_1$ values (all data) | 0.0733 | 0.0632 | 0.0949 | 0.0583 | 0.0439 |
| w$R_2$ values (all data) | 0.1909 | 0.1365 | 0.1991 | 0.1469 | 0.1185 |

**Structural comparison.**

As shown in figures 1-5, the molecular architectures of **1-5** are not comparable ((See supporting information, Fig. S11-13). Molecule **2** is a rare three dimensional lead carboxylate coordination polymer, while **1** and **3**-**5** are two dimensional layers with unique order. **1**-**5** are not comparable with known 3D Pb(II)-imidazolium carboxylate frame work, $[PbCl[\{HCN(CH_2COO)\}_2CH]_n$ reported by Wang *et al.*[8] The highly

diversified coordination numbers with flexible geometries are observed for the lead centers in **1-5**. Molecules **1**, **4** and **5** are constituted by octahedron, square pyramid and distorted cube, respectively. Notably, the molecule **2** is comprised of six different polyhedrons, while **3** is constructed by four different polyhedrons. These structural diversities can be attributed to the number of flexible nodes in ligand along with nature of carboxylate group as well as the reaction conditions.

**Solid-state UV-vis and fluorescent spectra of 1-5.**

The solid-state UV-visible absorption spectra of **1**-**5** are shown in figure 6. Compound **1** shows a broad absorption peak at 236 nm with very high intensity due to a strong ligand to metal charge transition, while **2**-**5** gave relatively a broad absorption band from 220 nm to 340 nm. A broad absorption peak observed from 236 to 309 nm can be attributed to the n-π* and π-π* transitions of ligand. Although **4** and **5** are originated by $\mathbf{L^3}$, the solid state UV-vis absorption spectra of **4** and **5** are not comparable; which clearly differentiate the structural diversity. Besides, the absorption intensity of **5** is much stronger than **4**.

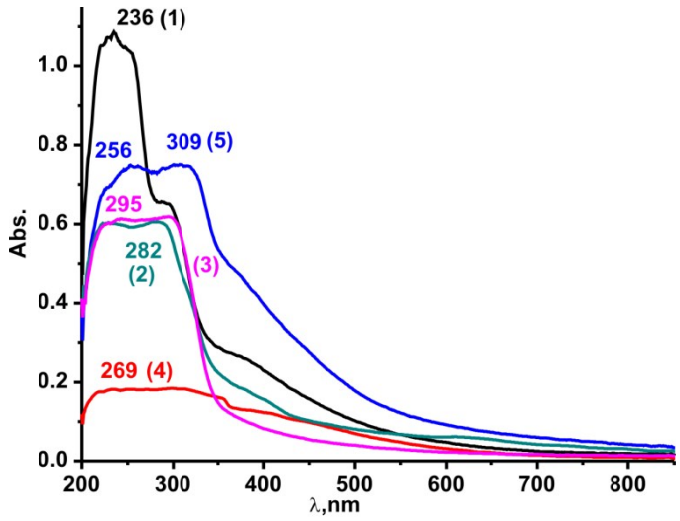


**Fig 6.** The solid state UV-vis absorption spectra of **1-5**.

The solid-state fluorescent emission spectra of **1–5** were measured at an excitation wavelength of 370 nm at room temperature (See supporting info, Fig. S14-S17). Molecules **1**-**5** shows a blue emission (**1** (438 nm), **2** (437), **3** (436), **4** (425) and **5** (434)). The emission intensity of **1, 2, 4** and **5** are almost comparable with corresponding ligands, **L**H (434 nm) and $\mathbf{L^1}H_2Br_2$ (436 nm), $\mathbf{L^3}H_2Cl$ (437 nm), respectively. Notably, the emission intensity of **3** is much stronger than ligand $\mathbf{L^2}H_2Br_2$ (435 nm).

**Thermogravimetric analysis of 1-5.**

The thermogravimetric analysis (TGA) of **1-5**, (10 °C $min^{-1}$, 30-1000 °C, under $N_2$ atmosphere) was carried out on **1-5** (Fig. 7). The TGA profile of **1** shows a minor weight loss (6% from 28 °C to 241 °C) then major weight loss (36% from 241 °C to 265 °C and 10% from 265 °C to 511 °C) due to the elimination of nitro group and L. The TGA analysis of **2** shows continues weight loss (~68%) from 180 °C to 1000 °C mainly due to the loss of bromide ion and $\mathbf{L^1}$. Molecule **3** follows three steps decomposition (from 50–245 °C with 4%weight loss, from 245 °C to 432 °C with 36% weight loss and from 432 °C to 638 °C with 27% weight loss). The total weight loss of 67% for **3** was mainly due to the loss of $\mathbf{L^2}$. The TGA profile of **4** depicts remarkable thermal stability. Then, the sample suffers incessant weight loss until it reaches a temperature of 673 °C. The total weight loss of 71% corresponds to the removal of the $\mathbf{L^3}$. Like **4**, **5** shows continue weight loss (from 45 °C to 780 °C with 79% weight loss) due to the loss of $\mathbf{L^3}$.

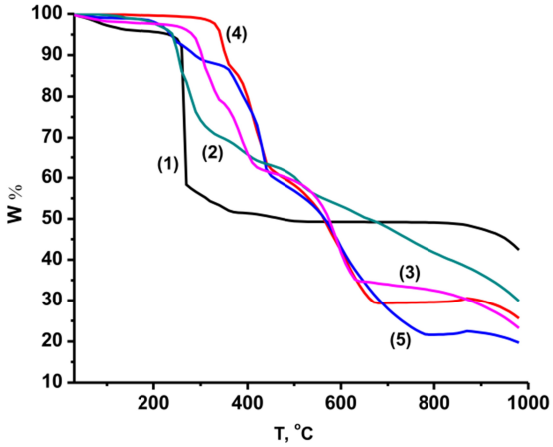


**Fig 7.** TGA curves of compounds **1-5** from 30 °C to 1000 °C with 10 °C $min^{-1}$ heating rate under $N_2$ atmosphere.

**Catalytic properties of 1-5.**

Over the past decade, various thiazolium, imidazolium and triazolium salts have been developed as organocatalysts for the benzoin condensation reaction under mild conditions with high selectivity. As a result, a large number of benzoin condensation processes have been well established using different types of NHCs.[10] In this paper, we attempted to use one mol% lead coordination polymers **1**-**5** as NHC-like catalysts for benzoin condensation reactions in toluene (Scheme 1, Supporting information 2, Figures S1-S5). The catalytic reactions were analysed with benzaldehyde under ambient temperature in the presence of four mol% potassium *tert*butoxide as base to activate imidazolium moieties in lead framework (Table 2). The reactions were carried out for 2 h to obtain the benzoin product with very good yield (75-88%, table 2, entries 1-5). As reported in entries 6-9 (Table 2), the benzoin condensation reaction was carried out using one mol% of insitu lead nitrate and imidazolium carboxylate ligands (**L**H, $\mathbf{L^1}H_2Br_2$, $\mathbf{L^2}H_2Br_2$ and $\mathbf{L^3}H_2Cl$) in the presence of four mol% potassium *tert*butoxide. Similarly, the reactions were studied using only ligands (**L**H, $\mathbf{L^1}H_2Br_2$, $\mathbf{L^2}H_2Br_2$ and $\mathbf{L^3}H_2Cl$) as organocatalysts. However, the yield of entries 6-17 is not appreciable compared to catalysts **1**-**5** (Table 2, entries 1-5) even after extending the reaction time for 12 h (48-60%, table 2, entries 6-17). In addition, the catalytic conversion was

absent, when the reaction was analysed using only lead nitrate (entry 18). Thus, the insitu generated carbene centres in coordination polymers **1**-**5** are responsible for the catalytic activities. Noteworthy that the catalytic efficiency of **1**-**5** is comparable with NHC (organocatalyst) mediated benzoin condensation reaction (See supporting information, Table S1).[10] As proposed for catalyst $[Co_3Cl_6(R'')_2]$, R" = 1,3,5-trimethylimidazole-2,4,6-triethylbenzene,[7] we assume that the molecular activation occurs on the surface of catalysts.

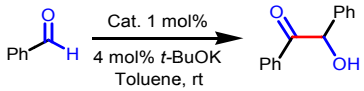


**Scheme 1.** Catalyst mediated benzoin condensation reaction in toluene at room temperature.

**Table 2.** The comparison of catalytic efficiency of **1**-**5** in toluene at room temperature.

| E | Cat. (1 mol%) | Time (h) | Isolated Yield (%)[a] |
|---|---|---|---|
| 1 | **1** | 2 | 78 |
| 2 | **2** | 2 | 88 |
| 3 | **3** | 2 | 84 |
| 4 | **4** | 2 | 80 |
| 5 | **5** | 2 | 75 |
| 6 | $Pb(NO_3)_2$ + **L**H | 12 | 58 |
| 7 | $Pb(NO_3)_2$ + $\mathbf{L^1}H_2Br_2$ | 12 | 60 |
| 8 | $Pb(NO_3)_2$ + $\mathbf{L^2}H_2Br_2$ | 12 | 56 |
| 9 | $Pb(NO_3)_2$ + $\mathbf{L^3}H_2Cl$ | 12 | 48 |
| 10 | **L**H | 2 | 20 |
| 11 | $\mathbf{L^1}H_2Br_2$ | 2 | 32 |
| 12 | $\mathbf{L^2}H_2Br_2$ | 2 | 28 |
| 13 | $\mathbf{L^3}H_2Cl$ | 2 | 30 |
| 14 | **L**H | 12 | 52 |
| 15 | $\mathbf{L^1}H_2Br_2$ | 12 | 60 |
| 16 | $\mathbf{L^2}H_2Br_2$ | 12 | 52 |
| 17 | $\mathbf{L^3}H_2Cl$ | 12 | 68 |
| 18 | $Pb(NO_3)_2$ | 24 | 0 |

[a]Determined by $^1$H NMR spectroscopy.

Moreover, **1**-**5** mediated catalytic conversion was further improved by extending the reaction time for 12 h (Fig. 8). Subsequently the catalytic reactions were extended for electron withdrawing group substituted aromatic aldehyde such as 4-nitro benzaldehyde (Scheme 2, Fig. 8). Catalysts **1**-**5** are very active towards benzoin condensation of 4-nitrobenzaldehyde. The catalytic reactions were repeated for three times and the yield is nearly comparable (See supporting information I, Table S2 and See supporting information II, Figures S14-S28). Notably, **1**-**5** are much superior than known (insitu) N-heterocyclic carbene mediated benzoin condensation of 4-nitrobenzaldehyde (See supporting information I, Table S3). Although, the catalysts **1**-**5** are very active (Yield, 88-99%), **1** gave excellent conversion for both benzaldehyde as well as 4-nitro benzaldehyde (Yield, 97-98%) (Fig. 8).

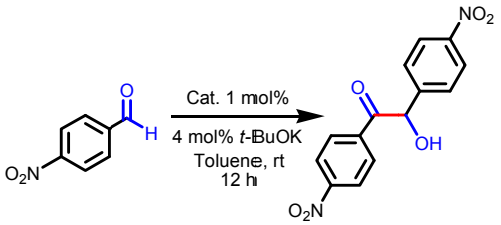


**Scheme 2.** Catalysts **1**-**5** mediated benzoin condensation of 4-nitrobenzaldehyde in 12 h.

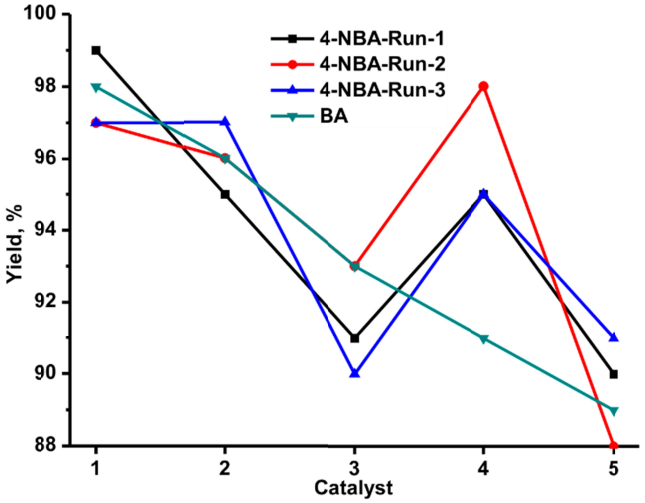


**Fig 8.** Catalysts **1**-**5** mediated benzoin condensation of benzaldehyde (BA, ◄) and 4-nitrobenzaldehyde (4-NBA, ■-run 1, ●-run 2, ▲-run 3) in 12 h. Yield was determined by $^1$H NMR spectroscopy.

Furthermore the functional group tolerance of **1** was evaluated for a range of substituted aromatic aldehydes (Scheme 3, Table 3 and Supporting information 1, Figures S6-S11). Catalyst **1** is highly active for 2-nitrobenzaldehyde (Table 3, entry 1), while 3-pyridinecarboxaldehyde (Table 3, entry 2), 4-fluorobenzaldehyde (Table 3, entry 3) and 4-chlorobenzaldehyde (Table 3, entry 4) gave considerable yield. Notably, the electron donating group substituted aromatic aldehydes such as 2-ethoxybenzaldehyde (Table 3, entry 5) and 4-ethylbenzaldehyde (Table 3, entry 6) depicted the poor yield.

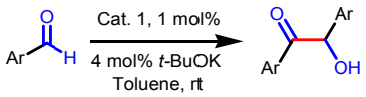


**Scheme 3.** Catalysts **1** mediated benzoin condensation of substituted benzaldehydes in 12 h.

**Table 3.** Evaluation of catalyst **1** scope.

| E | Substrate | Isolated yield (%)[a] |
|---|---|---|
| 1 | 2-Nitrobenzaldehyde | 92 |
| 2 | 3-Pyridinecarboxaldehyde | 75 |
| 3 | 4-Fluorobenzaldehyde | 60 |
| 4 | 4-Chlorobenzaldehyde | 50 |
| 5 | 2-Ethoxybenzaldehyde | 32 |
| 6 | 4-Ethylbenzaldehyde | 36 |

[a] Determined by $^1$H NMR spectroscopy.

## Experimental

### General Considerations

The solvents were purchased from commercial sources and purified according to standard procedures.[11] Unless otherwise stated, the chemicals were purchased from commercial sources. 2-(1-(carboxymethyl)-1*H*-imidazol-3-ium-3-yl)acetate (**L**H),[8] 3,3'-methylenebis(1-(4-carboxyphenyl)-1*H*-imidazol-3-ium) bromide ($\mathbf{L^1}H_2Br_2$)[4] and 1,3-bis(4-carboxyphenyl)imidazolium chloride ($\mathbf{L^3}H_2Cl$)[1] were prepared as previously reported method.[12] FT-IR measurement (neat) was carried out on a Bruker Alpha-P Fourier transform spectrometer. The UV–vis spectra were measured on a T90+ UV-visible spectrophotometer. The fluorescent spectra were measured on a Fluoromax-4P TCSPC, Horiba Scientific spectrophotometer. The thermogravimetric analysis (TGA) was performed using a TA-SDT Q600, Tzeropress. The suitable crystals **1**-**5** were selected and measured on a SuperNova, Dual, Cu at zero, Eos diffractometer. The crystal **3** was kept at 293 K, and **1**, **2**, **4** and **5** were kept at 150 K during data collection. Using Olex2, the structure was solved with the olex2.solve structure solution program using Charge Flipping and refined with the olex2.refine[13] refinement package using Gauss-Newton minimisation. Absorption corrections were performed on the basis of multi-scans.

The compound **2** was crystallized using water as solvent. Refinement without PLATON SQUEEZE showed severely disordered isolated solvent molecules in the structure which could not be modelled as discrete atomic sites.[14] The implementation of SQEEZE procedure on this structure using PLATON program showed the total void volumes approximately 1600Å$^3$ (15%) which contribute 625 electrons in the unit cell. The solvent free data set was used to remove the electronic contribution of disordered solvent molecules (water/nitrate) and the atoms used in the final model are reported in chemical formula and related parameters. Due to high (under corrected) absorption by Pb, the locating disordered atoms becomes guesswork. The Br is contaminated by Cl. The refinement with respect to relative contributions of Cl and Br in each site separately and gave 4.4 Br to 2.6 Cl per formula unit. This is a rather typical case of isomorphous substitution, as Cl and Br satisfy the two conditions set by Goldschmidt's rules (radii differing by <15% and similar type of bonding). Structure **3** showed four solvent accessible void volumes of 105 Å$^3$ which is approximately 7% in the total volume of the unit cell. Totally these void volumes contribute 32 electrons in the unit cell. The PLATON Squeeze program[14] was implemented to remove the electronic contributions of these disordered solvent molecules (either they may be water or nitrate anions) and only the atoms used in the final refined model is reported in chemical formula and related parameters. In structure **5**, one of the nitrate group is disordered. The reasonable behaviour of the nitrate was achieved by very harsh ISOR restraints.

Non-hydrogen atoms were anisotropically refined. Hydrogen atoms were included in the refinement in calculated positions riding on their carrier atoms. No restraint has been made for any of the compounds. The function minimized was $[\sum w(F_o^2 - F_c^2)^2]$ ($w = 1/[\sigma^2(F_o^2) + (aP)2 + bP]$), where $P = (\max(F_o^2,0) + 2F_c^2)/3$ with $\sigma^2(F_o^2)$ from counting statistics. The functions $R_1$ and $wR_2$ were $(\sum||F_o| - |F_c||)/\sum|F_o|$ and $[\sum w(F_o^2 - F_c^2)^2/\sum(wF_o^4)]^{1/2}$, respectively. CCDC 1423047-1423051 contains the supplementary crystallographic data for this paper. These data can be obtained free of charge from the Cambridge Crystallographic Data Centre via www.ccdc.cam.ac.uk/data_request/cif or from the Cambridge Crystallographic Data Centre, 12 Union Road, Cambridge CB2 1EZ, UK; fax: +44 1223 336 033; or e-mail: deposit@ccdc.cam.ac.uk.

### Synthesis of 3,3'-(ethane-1,2-diyl)bis(1-(4-carboxyphenyl)-1*H*-imidazol-3-ium) bromide ($\mathbf{L^2}H_2Br_2$)

A mixture of 1,2-dibromoethane (0.50 g, 2.69 mmol) and ethyl 4-(1H-imidazol-1-yl)benzoate (1.16 g, 5.38 mmol) in 1,4-dioxane (10 mL) was refluxed for 48 h. The solvent was filtered using cannula then the solid was washed with 1,4-dioxane (10 mL) and diethyl ether (10 mL). Solvent was removed under reduced pressure and dried under high vacuum. Then 12% HCl aqueous solution (30 mL) was added and refluxed for 3 h. The solvent was removed under reduced pressure and dried under high vacuum. Yield: 73% (based on ethyl 4-(1H-imidazol-1-yl)benzoate). M.p., 298 $^o$C (decomp.). HRMS (+ESI): calcd for $C22H19BrN4O4^+$ ([M–HBr]$^+$) 483.3147; found 483.0643. $^1$H NMR (400 MHz, DMSO-$d_6$): $\delta$ = 13.43 (bs, 2H, COO*H*), 10.34 (s, 2H, Im*H*), 8.46 (s, 2H, Ar*H*), 8.2 (m, 4H, Ar*H*), 8.08 (s, 2H, Ar*H*), 7.97 (s, 4H, Im*H*), 4.98 (s, 4H, C$H_2$) ppm. $^{13}$C NMR (100 MHz, DMSO-$d_6$): $\delta$ = 166.11 (C=O), 137.79 (Ar*C*), 136.86 (Im*C*), 131.77 (Ar*C*), 131.10 (Ar*C*), 123.72 (Im*C*), 121.84 (Ar*C*), 120.95 (Im*C*), 48.74 (*C*H$_2$) ppm. FT-IR (neat): $\bar{\upsilon}$ = 3290(w), 3016(w), 3356(w), 1712(s), 1604(m), 1548(s), 1425(w), 1330(w), 1272(s), 1226(s), 1189(m), 1113(m), 1063(m), 989(m), 956(m), 852(m), 791(w), 767(m), 670(w), 631(m) cm$^{-1}$.

### Synthesis of $[Pb(L)(NO_3)]_n$ (1)

To a mixture of **L**H (0.05 g, 0.27 mmol) and $Pb(NO_3)_2$ (0.18 g, 0.54 mmol), DMF (5 ml) was added. The reaction temperature was maintained at 120 $^o$C for two days then cooled to room temperature. Colourless crystals of **1** was obtained within 12 h. Yield: 70% (based on $Pb(NO_3)_2$). M.p., 230-232 $^o$C (decomp.). FT-IR (neat): $\bar{\upsilon}$ = 3111(w), 3080(w), 1642(w), 1555(s), 1389(s), 1308(s), 1166(m), 1103(w), 1028(w), 975(w), 926(w), 871(w), 800(w), 766(m), 706(s), 627(w), 595(w), 581(w) cm$^{-1}$.

### Synthesis of $[Pb_5(L^1)_2(NO_3)_2(Br)_{4.4}(Cl)_{2.6}(H_2O)]_n\cdot(NO_3)_2\cdot xH_2O$ (2)

A suspension of $\mathbf{L^1}H_2Br_2$ (0.05 g, 0.09 mmol), $Pb(NO_3)_2$ (0.06 g, 0.18 mmol) in water (5 ml) was preserved at 100 $^o$C for 12 h then slowly allowed to reach at room temperature. A large amount of colourless crystals of **2** was obtained within 12 h. Yield: 40% (based on $Pb(NO_3)_2$). M.p., 252-254 $^o$C. $^1$H NMR (400 MHz, DMSO-$d_6$): $\delta$ = 10.20 (s, 2H, Im*H*), 8.53 (s, 2*H*, ), 8.29 (s, 2H, Ar*H*), 8.23 (d, 4H, Ar*H*), 7.93 (d, 4H, Im*H*), 6.86 (s, 2H, C$H_2$) ppm. $^{13}$C NMR (100 MHz, DMSO-$d_6$): $\delta$ = 166.89 (C=O),

138.29 (Ar*C*), 137.92 (Im*C*), 131.75 (Ar*C*), 123.73 (Ar*C*), 122.60 (Ar*C*), 122.19 (Im*C*), 59.50 (*C*$H_2$) ppm. FT-IR (neat): $\bar{\upsilon}$ = 3356(w), 3103(w), 3030(w), 1696(s), 1647(w), 1607(m), 1549(m), 1422(m), 1394(s), 1343(m), 1321(s), 1304(s), 1214(s), 1121(m), 1069(m), 1037(w), 1014(w), 990(w), 954(w), 862(m), 826(w), 798(w), 768(s), 685(m), 649(w), 615(m) $cm^{-1}$.

**Synthesis of $[Pb_4(L^2)_2(NO_3)_8(H_2O)_4]_n \cdot xH_2O$ (3)**

A suspension of $L^2H_2Br_2$ (0.05 g, 0.09 mmol) and $Pb(NO_3)_2$ (0.06 g, 0.18 mmol) in water (3 ml) and DMF (2 ml) was maintained at 100 $^oC$ for 12 h then slowly brought to room temperature. The colourless crystals of **3** was obtained within 12 h. Yield: 45% (based on $Pb(NO_3)_2$). M.p., 279-282 $^oC$. FT-IR (neat): $\bar{\upsilon}$ = 3080(w), 1601(w), 1531(m), 1386(s), 1298(s), 1214(m), 1114(w), 1067(w), 1013(w), 849(s), 778(m), 722(w), 675(w), 636(m), 598(w) $cm^{-1}$.

**Synthesis of $[Pb(L^3)(Cl)]_n$ (4)**

A mixture of $L^3H_2Cl$ (0.05 g, 0.15 mmol) and $Pb(NO_3)_2$ (0.10 g, 0.29 mmol) in DMF (3 mL) was heated at 120 °C for 12 h under solvothermal condition. Yield: 54% (based on $Pb(NO_3)_2$). M.p., 290-292 $^oC$ (decomp.). FT-IR (neat): $\bar{\upsilon}$ = 3067(w), 1598(m), 1538(s), 1374(s), 1306(s), 1246(m), 1171(m), 1092(m), 1058(w), 1034(w), 1011(w), 950(w), 874(m), 845(s), 800(s), 741(m), 715(m), 696(s), 660(m), 617(m) $cm^{-1}$.

**Synthesis of $[Pb(L^3)(NO_3)]_n$ (5)**

$L^3HCl$ (0.05 g, 0.15 mmol), $Pb(NO_3)_2$ (0.10 g, 0.29 mmol) and DMF (5 ml) were loaded in a schlenk tube. Subsequently, the schlenk tube temperature was maintained at 120 $^oC$ for two days then slowly allowed to reach at room temperature. The colourless crystals of **5** were obtained within 12 h. Yield: 50% (based on $Pb(NO_3)_2$). M.p., 280-282 $^oC$ (decomp.). FT-IR (neat): $\bar{\upsilon}$ = 3093(w), 3057(w), 1608(m), 1579(m), 1545(s), 1512(m), 1430(w), 1353(s), 1312(s), 1252(s), 1156(m), 1133(m), 1062(m), 1008(m), 945(w), 862(m), 838(m), 774(s), 710(m), 685(m), 628(m) $cm^{-1}$.

**Reaction condition of benzoin condensation reactions**

Oven dried Schlenk was charged with catalysts (1 mol%), benzaldehyde (0.94 mmol) then dried under vacuum for 5 min. Solvent (5 mL) was added under nitrogen condition to the reaction mixture, evacuated for few seconds, refilled with nitrogen then KOt-Bu (4 mol%) was added to the reaction mixture under nitrogen condition at room temperature. The reaction progress was monitored by TLC. The reaction mixture was diluted with water (10 mL) and DCM (10 mL). The organic phase was separated, washed with brine solution (7 mL), dried over anhydrous sodium sulphate then the reaction mass was concentrated under reduced pressure to get crude compound. The crude compound was absorbed on silica gel (100-200 mesh) for purification then petroleum ether and 10% ethyl acetate/petroleum ether (200 mL) were poured on column to separate the final product.

## Conclusions

In conclusion, here we investigated the reaction between lead nitrate and different organic ligand systems based on the imidazolium carboxylate along with variable structural freedom at organic spacer. We have also shown that a novel structural topologies and versatile coordination properties could be achieved by changing the number of flexible node at organic spacer and employing judicious synthetic strategies. The first catalytic application of imidazolium carboxylate spacers supported lead assemblies has been explored. The present catalytic demonstration evidence that the catalysts **1**-**5** shows the high nucleophilic activity, facilitating a proton transfer, ability to stabilize negative charge in active aldehyde intermediate and ability to depart finally. Their catalytic applications in benzoin condensation reactions have been promising with different aldehydes. Structural insight into these compounds provides explanations for the diverse catalytic behaviours of these compounds. Future studies on the reactivity of these ligands and their heavier main-group metal complexes toward organic transformations are underway in our laboratory.

## Acknowledgements

We gratefully acknowledge the DST-FT (SR/FT/CS-94/2010) for financial support. CNB thank UGC for the fellowship.

## Notes and references

1 S. Sen, N. N. Nair, T. Yamada, H. Kitagawa and P. K. Bharadwaj, *J. Am. Chem. Soc.*, 2012, **134**, 19432.
2 (a) J. Y. Lee, J. M. Roberts, O. K. Farha, A. A. Sarjeant, K. A. Scheidt and J. T. Hupp, *Inorg. Chem.*, 2009, **48**, 9971; (b) G. Nickerl, A. Notzon, M. Heitbaum, I. Senkovska, F. Glorius and S. Kaskel, *Cryst.Growth Des.,* 2012, **13**, 198; (c) S. Wang, Q. Yang, J. Zhang, X. Zhang, C. Zhao, L. Jiang and C.-Y. Su, *Inorg. Chem.*, 2013, **52**, 4198; (d) S. Sen, S. Neogi, A. Aijaz, Q. Xu and P.K. Bharadwaj, *Inorg. Chem.*, 2014, **53**, 7591; (e) S. Sen, T. Yamada, H. Kitagawa and P.K. Bharadwaj, *Cryst. Growth Des.*, 2014, **14**, 1240.
3 (a) C. I. Ezugwu, N. A. Kabir, M. Yusubov and F. Verpoort, *Coord. Chem. Rev.*, 2015, *in press and references therein*; (b) J. Lee, O. K. Farha, J. Roberts, K. A. Scheidt, S. T. Nguyen and J. T. Hupp, *Chem. Soc. Rev.,* 2009, **38**, 1450.
4 G-Q. Kong, X. Xu, C. Zou and C.-D. Wu, *Chem. Commun.*, 2011, **47**, 11005.
5 G.-Q. Kong, S. Ou, C. Zou and C.-D. Wu, *J. Am. Chem. Soc.*, 2012, **134**, 19851.
6 A. Burgun, R. S. Crees, M. L. Cole, C. J. Doonan and C. J. Sumby, *Chem. Commun.*, 2014, **50**, 11760.
7 M. B. Lalonde, O. K. Farha, K. A. Scheidt and J. T. Hupp, *ACS Catal.*, 2012, **2**, 1550.
8 X. W. Wang, L. Han, T-J. Cai, Y-Q. Zheng, J-Z. Chen and Q. Deng, *Crystal Growth & Design.,* 2007, **7**, 1027.
9 K. Nakamoto, Infrared and Raman Spectra of Inorganic and Coordination Compounds, Part B: Applications in Coordination, Organometallic and Bioinorganic Chemistry, 6th Ed.; John Wiley & Sons, Inc. New Jersey, 2009.
10 For selected examples of NHC mediated Benzoin Condensation reaction: (a) D. Enders, O. Niemeier and A. Henseler, *Chem. Rev.,* 2007*,* **107**, 5606; (b) I. Piel, M. D.

Pawelczyk, K. Hirano, R. Fröhlich and F. Glorius, *Eur. J. Org. Chem.,* 2011, 5475; (c) Y. He and Y. Xue, *J. Phys. Chem.,* 2011, **115**, 1408; (d) S. M. Langdon, M. M. D. Wilde, K. Thai and M. Gravel, *J. Am. Chem. Soc.*, 2014, **136**, 7359; (e) L. Baragwanath, C. A. Rose, K. Zeitler and S. J. Connon, *J. Org. Chem*., 2009, **74**, 9214; (f) D. Enders and U. Kallfass, *Angew. Chem. Int. Ed*., 2002, **41**, 1743; (g) A. Satyanarayana and G. Prabusankar, *J. Chem. Sci.,* 2015, **127**, 821; (g) Y. Ma, S. Wei, J. Wu, F. Yang, B. Liu, J. Lan, S. Yang and J. You, *Adv. Synth. Catal*., 2008, **350**, 2645.

11 D. D. Perrin and W. L. F. Armarego, *Purification of Laboratory Chemicals*, *3rd Ed.,* Pergamon Press, London, 1988.

12 (a) P. Suresh, A. Samanta, A. Sathyanarayana and G. Prabusankar, *J. Mol. Struct.*, 2012, **1024**, 170; (b) P. Suresh, S. Radhakrishnan, C. N. Babu, A. Sathyanarayana, N. Sampath and G. Prabusankar, *Dalton Trans.*, 2013, **42**, 10838; (c) K. Srinivas, C. N. Babu and G. Prabusankar, *Dalton Trans.*, 2015, **44**, 15636.

13 O. V. Dolomanov, L. J. Bourhis, R. J. Gildea, J. A. K. Howard and H. Puschmann, OLEX2: a complete structure solution, refinement and analysis program. *J. Appl. Cryst.,* 2009, **42**, 339.

14 A. L. Spek, *Acta Cryst*., 2015, **C71**, 9-18.